Am J Physiol Heart Circ Physiol
279: H1120–H1127, 2000.

Left ventricular wall stress normalization in chronic pressure-overloaded heart: a mathematical model study

PATRICK SEGERS,[1] NIKOS STERGIOPULOS,[2] JAN J. SCHREUDER,[3]
BEREND E. WESTERHOF,[4] AND NICO WESTERHOF[1]
[1]*Laboratory for Physiology, Institute for Cardiovascular Research, Free University of Amsterdam, and* [4]*Biomedical Instrumentation, Institute of Applied Physics, Netherlands Organization for Applied Scientific Research, Academic Medical Center, 1081 BT Amsterdam, The Netherlands;* [2]*Biomedical Engineering Laboratory, Ecole Polytechnique Fédéralé de Lausanne, 1015 Lausanne, Switzerland; and* [3]*Department of Cardiac Surgery, Ospedale San Raffaele, 20132 Milan, Italy*

Received 12 August 1999; accepted in final form 2 March 2000

Segers, Patrick, Nikos Stergiopulos, Jan J. Schreuder, Berend E. Westerhof, and Nico Westerhof. Left ventricular wall stress normalization in chronic pressure-overloaded heart: a mathematical model study. *Am J Physiol Heart Circ Physiol* 279: H1120–H1127, 2000.—It is generally accepted that the left ventricle (LV) hypertrophies (LVH) to normalize systolic wall stress (σ_s) in chronic pressure overload. However, LV filling pressure (P_v) may be elevated as well, supporting the alternative hypothesis of end-diastolic wall stress (σ_d) normalization in LVH. We used an LV time-varying elastance model coupled to an arterial four-element lumped-parameter model to study ventricular-arterial interaction in hypertension-induced LVH. We assessed model parameters for normotensive controls and applied arterial changes as observed in hypertensive patients with LVH (resistance +40%, compliance −25%) and assumed *1*) no cardiac adaptation, *2*) normalization of σ_s by LVH, and *3*) normalization of σ_s by LVH and increase in P_v, such that σ_d is normalized as well. In patients, systolic and diastolic blood pressures increase by ~40%, cardiac output (CO) is constant, and wall thickness increases by 30–55%. In *scenarios 1* and *2*, blood pressure increased by only 10% while CO dropped by 20%. In *scenario 2*, LV wall thickness increased by only 10%. The predictions of *scenario 3* were in qualitative and quantitative agreement with in vivo human data. LVH thus contributes to the elevated blood pressure in hypertension, and cardiac adaptations include an increase in P_v, normalization of σ_s, and preservation of CO in the presence of an impaired diastolic function.

hypertrophy; heart-arterial interaction; aging; hypertension; varying elastance; windkessel; left ventricle

THE FACT THAT THE HEART and the arterial system make an interacting pair is most obvious in conditions of chronic pressure overload, where the complex interaction of the heart and arterial system leads to changes in blood pressure. Altered arterial system properties affect blood pressure and cardiac output; this change in blood pressure, in turn, affects the heart.

The generally accepted concept is that, as a response to chronic pressure overload, the left ventricle (LV) hypertrophies to compensate for increased systolic wall stress by increasing its wall thickness; i.e., wall stress is maintained at normal values (11). The increase in pump function then allows for the generation of a normal cardiac output against higher loads (9). However, this straightforward adaptive pattern is not always observed in experimental animal studies with induced chronic pressure overload. Frequently, an elevation of LV end-diastolic pressure is found that is moderate in absolute value (a few mmHg) but significant in a relative sense and is of the same order of magnitude as the relative increase in LV wall thickness (2, 10, 13, 19, 22, 24, 26, 29). This observation led to the hypothesis that LV end-diastolic wall stress is normalized in chronic pressure overload (22, 26) or that end-diastolic and systolic wall stress are normalized (10, 29).

We have used a mathematical model (31) to study the heart-arterial interaction in conditions of chronic pressure overload, i.e., essential hypertension, where total peripheral resistance is increased and total arterial compliance is decreased compared with normotensive controls (9, 30). With implementation of these arterial changes, LV pressure-volume (P-V) loops and aortic pressure and flow waves are calculated according to three heart-arterial interaction scenarios: *1*) there are no cardiac changes in response to the increased load; *2*) peak systolic wall stress is normalized via an increase in LV wall thickness; and *3*) peak systolic wall stress is normalized through an increase in LV wall thickness, and LV end-diastolic pressure is allowed to change to normalize end-diastolic wall stress. A mathematical model allowed us to simulate hypothetical conditions that are actually impossible to obtain in the in vivo setting, yielding more insight into the structural changes that must occur to explain hypertension-induced alterations in systolic and end-diastolic wall stress. As such, the contribution of the heart in chronic pressure overload and the importance of the

Address for reprint requests and other correspondence: P. Segers, Laboratory for Physiology, Institute for Cardiovascular Research, Free University of Amsterdam, van der Boechorststraat 7, 1081 BT Amsterdam, The Netherlands (E-mail: segers@physiol.med.vu.nl).

The costs of publication of this article were defrayed in part by the payment of page charges. The article must therefore be hereby marked "*advertisement*" in accordance with 18 U.S.C. Section 1734 solely to indicate this fact.

elevated LV filling pressure can be assessed. This study further addresses whether the views on normalization of systolic and end-diastolic wall stress in the chronic pressure-overloaded heart can be merged.

MATERIALS AND METHODS

Heart-Arterial Model

The heart-arterial model consists of a time-varying elastance model [$E(t)$] (34) coupled to a four-element lumped-parameter windkessel model representing the arterial load (33). It has been shown that, after normalization of the elastance curve to peak elastance (E_{max}; $E_N = E/E_{max}$) and time (t) to the time to reach peak elastance (t_P; $t_N = t/t_P$), this normalized time-varying elastance curve [$E_N(t_N)$], measured in healthy subjects and in patients with various cardiovascular diseases, always has the same shape (28, 34). The elastance curve given by Senzaki et al. (28) is for a signal with period $t_N = 3.46$. To obtain periodicity for shorter cycles (<3.46), $E_N(t_N)$ is rotated around $E_N(0)$ to give the start and the end of the cardiac cycle the same value. Furthermore, $E_N(t_N)$ is set to E_{min}/E_{max} for all points after isovolumic relaxation (Fig. 1), where E_{min} is minimal elastance. This linearizes the passive diastolic pressure-volume (P-V) relationship. $E(t)$ is then fully described by three parameters: E_{max}, E_{min}, and t_P. Other heart-related parameters are heart period (T), venous filling pressure (P_v), and the intercept of the end-systolic P-V relation with the volume axis (V_d) (34). In diastole, the heart fills through the mitral valve that is, in the open position, modeled as a linear resistance (0.001 mmHg·ml^{-1}·s).

The arterial model is a four-element lumped-parameter windkessel model (33) consisting of total peripheral resistance (R), total arterial compliance (C), total blood inertance (L), and the characteristic impedance of the aorta (Z_0; Fig. 1). To allow the coupling between the time-varying elastance model and the lumped-parameter arterial model, an inverse Fourier algorithm (Matlab 5.2, Mathworks) is used to transform the frequency domain description of the arterial model, i.e., the input impedance, into its time domain formulation, i.e., its impulse response function (3).

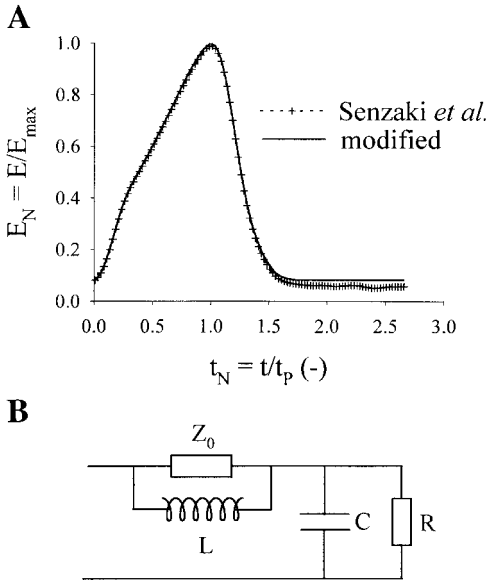

Fig. 1. *A*: original normalized time-varying elastance curve [$E_N(t_N)$] as given by Senzaki et al. (28) and modified $E_N(t_N)$ [for heart period (T) = 0.8 s and time to peak elastance (t_P) = 0.3 s]. E_{max}, peak elastance. *B*: arterial 4-element lumped-parameter model consisting of total peripheral resistance (R), total arterial compliance (C), aortic characteristic impedance (Z_0), and inertia (L).

An iteration loop starts at the onset of isovolumic contraction ($t = 0$). At that moment, LV pressure (P_{LV}) equals P_v, LV volume (V_{LV}) equals end-diastolic volume (LVEDV), and $E(t = 0) = E_{min}$ follows from the relation

$$E_{min} = \frac{P_v}{LVEDV - V_d}$$

As the ventricle contracts isovolumically, P_{LV} rises until an initially assumed end-diastolic aortic pressure (DBP_{ao}) is reached. Then the aortic valve opens and the heart starts to eject. At each time step, aortic flow ($\dot{Q}$) is determined, such that the increase in aortic pressure (P_{ao}), relative to DBP_{ao}, matches the increase in P_{LV}, which, in turn, is given by

$$E(t) = \frac{P_{LV}(t)}{V_{LV}(t) - V_d}$$

with $V_{LV}(t)$ calculated from LVEDV and $\dot{Q}$ from the previous time steps. End systole is reached as soon as $\dot{Q}(t)$ becomes negative, and it is assumed that $\dot{Q} = 0$ in diastole. At the end of the first iteration cycle, a new DBP_{ao} is obtained and a new cycle is calculated. The iteration continues until the difference in DBP_{ao} between two successive iteration loops is <1%. The iteration scheme was validated by comparison with results from an existing heart-arterial model (31), both models yielding identical results. The model has been programmed in Matlab 5.2 (Mathworks).

Validation of the Heart-Arterial Model

Other heart-arterial interaction models, similar to the model used in this study, have been validated earlier with data measured in the isolated canine (15) or feline (31) heart pumping into an artificial load. To test our model in the intact human cardiovascular system, we first compared model-generated data with data from three patients with dilated cardiomyopathy (27). A dual-micromanometer transducer conductance catheter (model F7, Sentron) was inserted via the femoral artery into the LV for measurement of P_{LV}, P_{ao}, and V_{LV}. The conductance catheter was connected to a Leycom Sigma-5DF signal conditioner/processor (CardioDynamics, Zoetermeer, The Netherlands) to measure V_{LV}. A Swan-Ganz thermodilution catheter was placed in the pulmonary artery for measurement of cardiac output and used for calibration of V_{LV} as measured by the conductance catheter. Further details on patients and protocols can be found elsewhere (27). Multiple beats ($n > 10$) at baseline were averaged to yield a single representative data set (Fig. 2). Differentiation of V_{LV} during systole gives an approximation of flow. V_d is assumed to be 15 ml for all patients. The P-V loop yields P_v and LVEDV and, thus, E_{min}. The remaining two parameters, E_{max} and t_P, are chosen to match measured and model $E(t)$. T is obtained from the electrocardiogram. Arterial parameters are derived from P_{ao} and $\dot{Q}$: R is calculated as $P_{ao}/\dot{Q}$, C is estimated using the pulse pressure method (32), and Z_0 is derived from the slope of $\dot{Q}$-P_{ao} in early systole (16). P_{LV}, V_{LV}, P_{ao}, and $\dot{Q}$ are computed using the heart-arterial model and are compared with the measured data.

Simulation of (Compensated) Cardiac Adaptation to Chronic LV Pressure Overload

Values for arterial and cardiac model parameters for control subjects and for hypertensive patients with concentric hypertrophy are taken from the literature. The data pre-

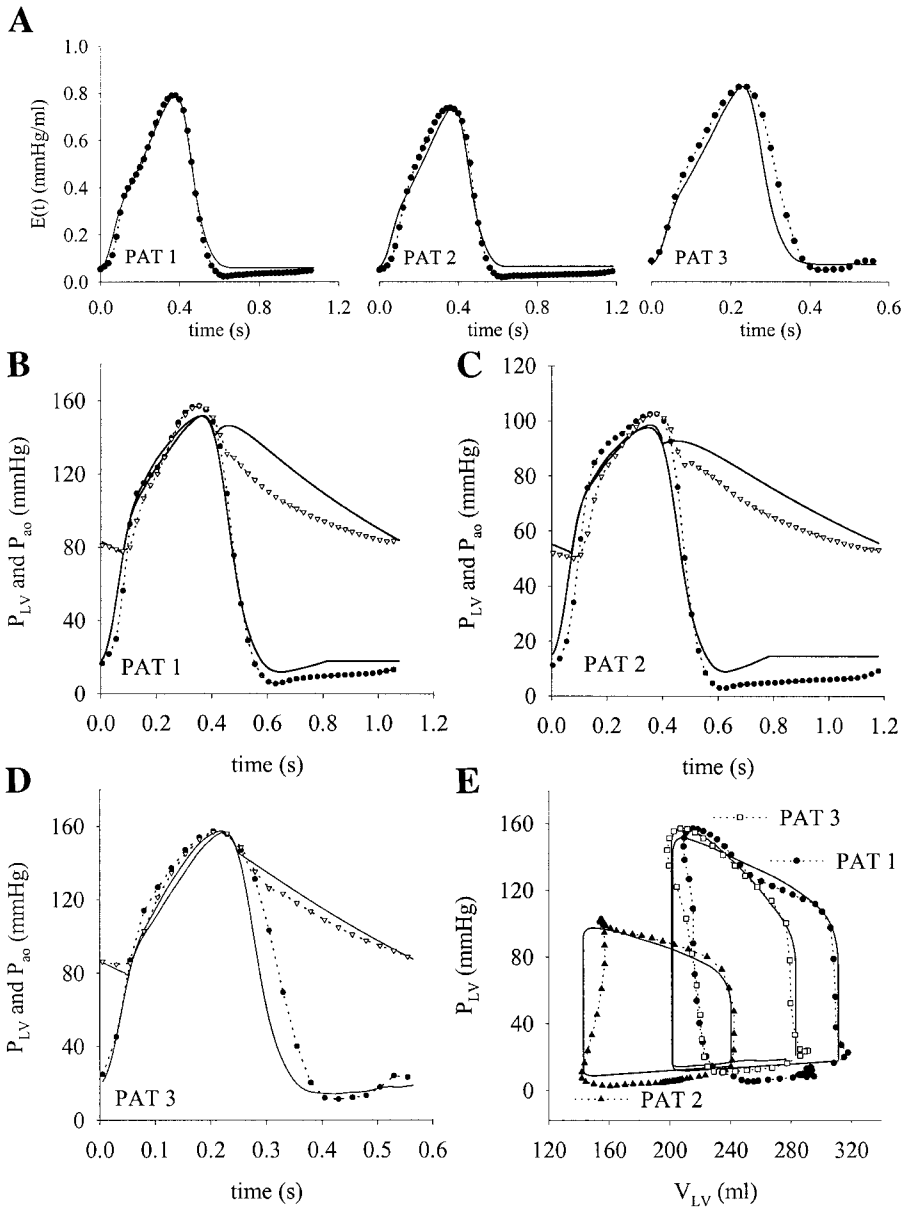

Fig. 2. *A*: ●, calculated time-varying elastance curve [$E(t)$] with diastolic volume (V_d) = 15 ml and measured left ventricular (LV) pressure and volume (V_{LV}) in *patients 1, 2,* and *3* (Pat 1, Pat 2, and Pat 3, respectively); line, modified $E(t)$ used in model with parameters from Table 1. *B–D*: comparison of measured left ventricular (P_{LV}; ▽) and aortic pressure (P_{ao}; ●) with simulations (lines) for *patients 1–3* by use of parameters from Table 1. *E*: comparison of measured (symbols) and simulated (lines) LV pressure-volume loops for *patients 1–3*.

dicted by the different scenarios are compared with data given by Ganau et al. (9), who give hemodynamic data averaged for a control group and for a patient population with concentric LV hypertrophy.

Model parameters for the normotensive subject. Control values for R and C are taken as 1.1 mmHg·ml^{-1}·s and 1.1 ml/mmHg (9), respectively. Z_0 = 0.033 mmHg·ml^{-1}·s^{-1} (21), and L is set to 0.005 mmHg·ml^{-1}·s^{-1} (33). T is taken to be 0.86 s (70 beats/min), and t_P = 0.32 s. E_{max} is 1.5 mmHg/ml, P_v is set to 5 mmHg, and V_d = 15 ml, giving E_{min} = 0.031 mmHg/ml.

Modeling chronic pressure overload (hypertension). Arterial changes in hypertension are modeled as a 25% decrease in C (0.82 ml/mmHg) and a 40% increase in R (1.54 mmHg·ml^{-1}·s) (9, 30). Z_0 varies in proportion to $1/\sqrt{C}$ and increases by 15% to 0.038 mmHg·ml^{-1}·s^{-1}.

Three heart-arterial coupling scenarios are considered: *1*) cardiac parameters do not vary; *2*) peak systolic wall stress (σ_s) is normalized via an increase in LV wall thickness; and *3*) peak σ_s is normalized through an increase in LV wall thickness, and P_v is allowed to change to normalize diastolic wall stress (σ_d). The σ_s and σ_d are calculated using the Laplace formula for a thick-walled sphere (18): $\sigma = Pr^2/h(2r + h)$, where r and h represent LV cavity radius and wall thickness, respectively, and P is P_{LV} at the moment of peak systolic pressure and end diastole (P_v), respectively. The radius is calculated from V_{LV} with the assumption of a spherical ventricular shape. Wall thickness for the control condition is taken as 1.6 cm. For an average V_{LV} of 150 ml, this yields an LV cavity-to-LV wall volume ratio of 0.44, which is within the normal range of 0.15–0.70 (1). For the control case, σ_s and σ_d are 11.7 and 0.6 kPa, respectively, and these values are used as the level to which stress is normalized in hypertension. Inasmuch as the LV P-V relations in systole and diastole are proportional to wall thickness, derived parameters E_{max} and E_{min} are proportional to wall thickness as well. Simulated data are presented as P_{LV}, P_{ao}, $\dot{Q}$, and P-V loops.

RESULTS

Validation of the Heart-Arterial Model

The parameters used for the simulation of the patient data are summarized in Table 1. For these dilated

hearts, LVEDV is high and varies from 240 to 311 ml, whereas P_v was between 14.6 and 19.3 mmHg. With V_d = 15 ml, this yields E_{min} between 0.060 and 0.072 mmHg/ml. E_{max} as estimated from the P-V relations is ~0.8 ml/mmHg. C is estimated to be between 0.68 and 1.32 ml/mmHg and Z_0 between 0.035 and 0.109 mmHg·ml^{-1}·s^{-1}. R is between 0.82 and 1.15 mmHg·ml^{-1}·s. With the model parameters from Table 1, the model elastance function is reasonably close to the calculated elastance curve by use of measured P_{LV} and V_{LV}, and V_d = 15 ml (Fig. 2*A*). Differences between measured and model-predicted systolic and diastolic pressure are −3 and −1%, respectively, for *patient 1*, −4.8 and +4% for *patient 2*, and 0 and −7% for *patient 3*. In systole, the correspondence between measured and calculated aortic and LV pressure data is good; in diastole, the discrepancy is larger, especially for *patients 1* and *2* (Fig. 2, *B–D*). Overall, the LV P-V loops are reasonably well simulated, especially during the ejection phase (Fig. 2*E*).

Simulation of (Compensated) Cardiac Adaptation to Chronic LV Pressure Overload

When cardiac parameters are kept constant (*scenario 1*), the arterial changes in hypertension lead to an increase in systolic (from 124 to 143 mmHg) and diastolic blood pressure (from 76 to 90 mmHg; Fig. 3). Stroke volume is predicted to decrease by 18% (from 80 to 65 ml), and peak flow is reduced as well as the duration of LV ejection (Fig. 3, *A* and *B*). Inasmuch as preload is unchanged, end-diastolic volume is constant, while end-systolic LV volume is increased (Fig. 3*C*).

The results for *scenario 2*, where LV wall thickness is increased to normalize peak σ_s, are shown in Fig. 3, *D–F*. Aortic systolic and diastolic pressures are ~5 mmHg lower than in *scenario 1*, and stroke volume is further depressed (63 ml), mainly because of the lower end-diastolic volumes (E_{min} increases and filling pressure remains the same). To normalize σ_s, wall thickness (and accordingly E_{max} and E_{min}) has increased by 10%.

Table 1. *Model parameters from patient data*

	Patient 1	*Patient 2*	*Patient 3*
Gender	M	M	M
Age, yr	64	56	65
Weight, kg	80	74	80
HR, beats/min	56	51	106
LVEDV, ml	311	240	283
P_v, mmHg	17.8	14.1	19.2
E_{max}, mmHg/ml	0.80	0.74	0.82
t_P, s	0.38	0.38	0.23
V_d, ml	15	15	15
Z_0, mmHg·ml^{-1}·s^{-1}	0.109	0.056	0.035
L, mmHg·ml^{-1}·s^{-2}	0.005	0.005	0.005
R, mmHg·ml^{-1}·s	1.15	0.94	0.82
C, ml/mmHg	0.87	1.32	0.68

Heart rate (HR), left ventricular end-diastolic volume (LVEDV), and venous filling pressure (P_v) were directly measured; peak elastance (E_{max}) and time to E_{max} (t_P) were determined from pressure-volume (P-V) loops by fit; the intercept of the end-systolic P-V relation (V_d) and inertance (L) were taken from the literature (31); characteristic impedance of aorta (Z_0), peripheral resistance (R), and arterial compliance (C) were estimated from aortic pressure and flow.

Figure 3, *G–I*, shows P_{ao} and $\dot{Q}$ and LV P-V relations when σ_s is normalized by an increase in wall thickness and when σ_d is normalized by an increase in preload (P_v), i.e., *scenario 3*. Diastolic (108 mmHg) and systolic (172 mmHg) blood pressure have increased by ~40%, while stroke volume and cardiac output are preserved (−0.4%). Wall thickness has increased by 34%, and P_v has risen from 5.0 to 6.9 mmHg (+38%). The effects of the different heart interaction scenarios on systolic and diastolic blood pressure and on cardiac output are summarized in Fig. 4, where a comparison with data (9) measured in normotensive controls (n = 125) and in hypertensive patients with compensated concentric hypertrophy (n = 13) is shown.

DISCUSSION

In the present study we used a theoretical model to study the interaction between the LV and the systemic circulation in conditions of chronic pressure overload as observed in hypertensive patients with compensated concentric hypertrophy. We assumed arterial compliance to be 25% lower and peripheral resistance to be 40% higher in hypertensive patients than in normotensive controls (30) and predicted blood pressure, cardiac output, LV filling pressure, and wall thickness according to three cardiac adaptation scenarios. The scenario where LV hypertrophy normalizes peak systolic wall stress and preload increases to normalize end-diastolic wall stress presented results most in line with data in the literature. The increase in systolic and diastolic blood pressure and the preservation of cardiac output are in qualitative and quantitative agreement with in vivo measurements (Fig. 4), and the 33% increase in wall thickness approximates that (30–55%) observed in patients with essential hypertension (30).

We used a relatively simple model, consisting of an LV time-varying elastance model coupled to an arterial lumped-parameter model, to simulate hemodynamics in the intact human. It was shown earlier that similar models generate pressure, flow, and P-V curves that are in good agreement with data measured in the isolated canine (15) or cat (31) heart pumping into an artificial load. Data necessary for a validation study of the model in humans (simultaneously measured LV pressure and volume and aortic pressure and flow) are, to the best of our knowledge, not available, especially not in healthy control subjects. Thus we could compare model predictions only with data that were measured in three patients with LV dilated cardiomyopathy before surgical treatment by cardiomyoplasty (27). Measured and simulated data are in good agreement, especially in systole, and our findings support the further application of the model for simulations on the hemodynamic interaction between the LV and the arterial load.

The shape of the normalized LV time-varying elastance curve for the dilated cardiomyopathy patients closely resembled $E_N(t_N)$ given by Senzaki et al. (28). Therefore, especially during the ejection phase, measured and model $E(t)$ curves are close (Fig. 2*A*). In diastole, the difference between measured and modeled $E(t)$ is somewhat larger, and this results in differ-

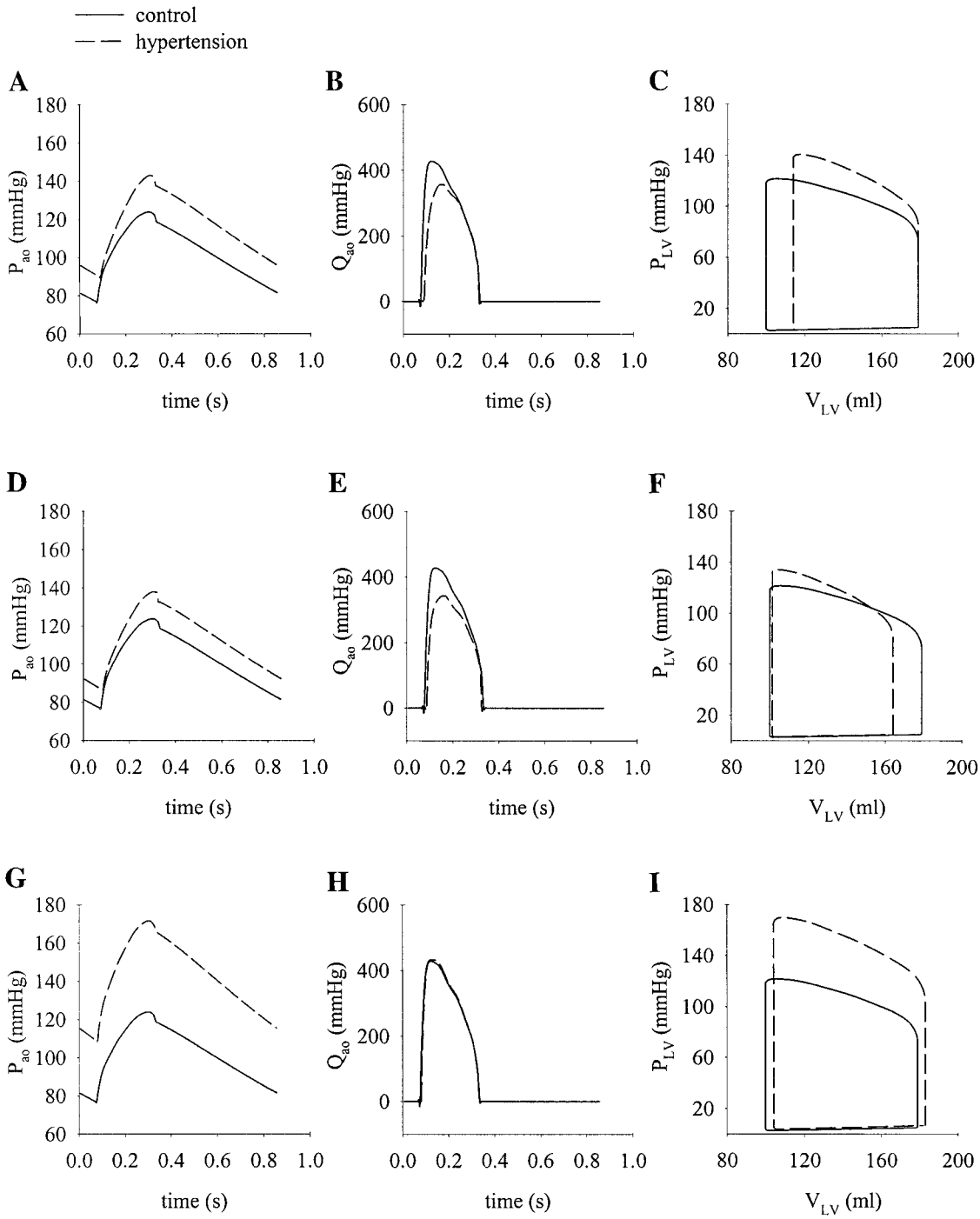

Fig. 3. P_{ao} (*A*, *D*, and *G*), aortic flow ($\dot{Q}_{ao}$; *B*, *E*, and *H*), and left ventricular pressure-volume loops (*C*, *F*, and *I*) with the arterial effects of hypertension modeled as a 25% decrease in compliance and a 40% increase in resistance. In *A–C,* cardiac parameters are kept constant; in *D–F*, wall thickness (via E_{max} and E_{min}) is modified to normalize peak systolic wall stress; and in *G–I,* wall thickness (via E_{max} and E_{min}) is modified to normalize peak systolic wall stress, and preload (venous filling pressure) is changed to normalize end-diastolic wall stress.

ences between measured and simulated LV pressures. However, part of this discrepancy also results from the simple model that was used for LV filling: LV pressure is calculated from LV volume via the elastance curve, and the time course of LV filling therefore determines the time course of LV pressure in diastole.

There is some discrepancy between measured and simulated aortic pressure during diastole in *patients 1* and *2*. This is the consequence of our choice of a linear four-element windkessel model as afterload. A (nonlinear) three-element windkessel model (36) with appropriately chosen model parameters may, for these patients, yield aortic pressure waves better resembling the measured data. These three-element windkessel models, however, have the disadvantage that the characteristic impedance is placed in series with the two-

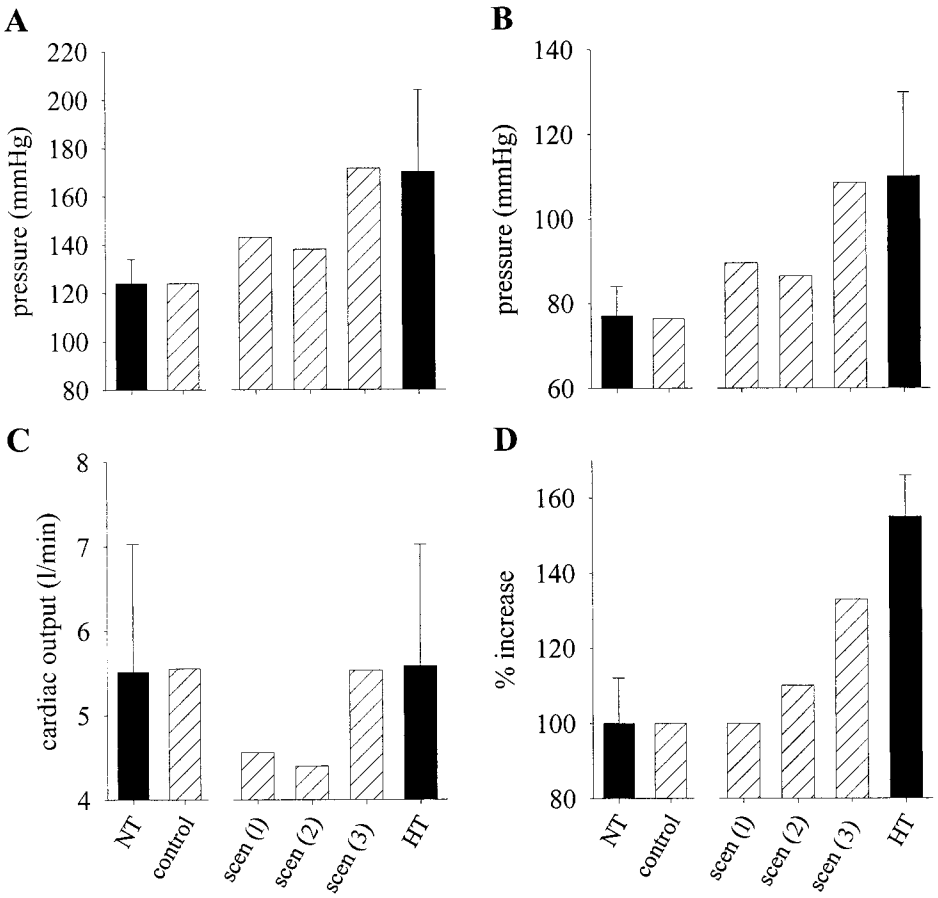

Fig. 4. Comparison of model simulations (hatched bars) with in vivo-measured (solid bars; means ± SD) systolic blood pressure (*A*), diastolic blood pressure (*B*), cardiac output (*C*), and left ventricular wall thickness increase (*D*) in normotensive controls (NT; $n = 125$) and in hypertensive patients with concentric hypertrophy (HT; $n = 13$; data from Ref. 9). Simulated data consist of the control condition and the results obtained with the 3 cardiac adaptation scenarios (seen): *1*) no cardiac changes, *2*) peak systolic wall stress normalization, and *3*) systolic wall stress normalization and change in venous filling pressure to normalize end-diastolic wall stress.

element windkessel model, necessitating correction factors on measured compliance and Z_0 to obtain a good fit of the actual input impedance (3, 33). The discussion on which lumped-parameter model best describes arterial input impedance is outside the scope of this work. In addition, lacking a high-fidelity flow wave measurement, we have insufficient detailed information to correctly answer this question.

LV wall stress normalization in compensated hypertrophy is used as a mechanism to explain LV hypertrophy in the presence of an increased load (11). An increased load results in higher systolic blood pressure and, following Laplace's law, leads to an increased wall stress. To reduce wall stress back to normal levels, we increased LV wall thickness, keeping LV internal diameter (at maximal systolic pressure) constant (concentric hypertrophy). The resulting increase in mass thus reflects a larger number of sarcomeres in parallel in the same number of myocytes. If possible intrinsic contractility changes due to altered calcium handling in hypertrophy are neglected (17, 20, 22), active contractile properties of the LV (E_{max}) vary in proportion to the increase in LV mass. On the other hand, the greater wall thickness will influence the passive diastolic P-V relation (E_{min}), inasmuch as higher pressures are needed to fill the stiffer ventricle. We thus assumed that E_{min} changes in proportion to E_{max}, and this assumption is supported by human studies reporting parallel changes in E_{max} and E_{min} (6, 17). There is further evidence, based on Doppler and ultrasound measuring techniques, that diastolic function is impaired in hypertension. Delayed LV diastolic relaxation has been reported (8, 17) as well as changes in the flow velocity pattern measured over the mitral valve during LV filling. The amplitude of the rapid early filling wave (E wave) is reduced, and the ratio of the E wave to the A wave (the A wave is a second peak in the LV filling wave due to contraction of the left atrium) is reduced (8, 14).

In the scenario where peak systolic LV wall stress was normalized to compensate for the increased afterload, blood pressure and wall thickness increased by only 10%. The main effect was a reduction in cardiac output due to the stiffer ventricle in diastole, while LV filling pressure remained at the same level. End-diastolic wall stress thus decreased, as end-diastolic pressure was constant, end-diastolic chamber dimensions were reduced, and wall thickness was increased. Therefore, LV wall stress normalization alone cannot account for the hemodynamic observations in hypertensive patients with LV hypertrophy.

Normalization of systolic wall stress is not always observed in experiments on chronic pressure-overloaded hearts. In dogs with an aortic constriction, Sasayama et al. (26) reported normalized end-diastolic wall stress after 18 days of chronic pressure overload but no normalized systolic wall stress. In dogs with renovascular hypertension, end-diastolic but not end-systolic wall stress

appears normalized (22), whereas in dogs with perinephritic hypertension, it has been reported that end-diastolic and end-systolic wall stress are normalized (10, 29).

When we allowed venous filling pressure to rise to normalize end-diastolic wall stress while still normalizing systolic wall stress, the hemodynamic data better matched the in vivo observations, with a marked elevation of systolic and diastolic pressure. For unaltered LV dimensions, wall thickness and venous filling pressure are increased by ~40%. This increase in wall thickness is within the range reported in hypertensive patients with concentric hypertrophy (9). Also, stroke volume and cardiac output are preserved, as reported elsewhere (9, 30). An increased venous filling pressure in the presence of an increased arterial load was observed earlier in animals in renovascular (22) and perinephrinic (10, 29) hypertension. In humans, elevated filling pressures have been reported in LV hypertrophy patients (2, 17). Indirect evidence is found in studies reporting on regression of venous filling pressure in aortic stenosis patients after valve replacement (12, 19). Pulmonary venous pressure is often increased in patients with acute LV dysfunction. In a theoretical model study, Burkhoff and Tyberg (5) showed that the increase in venous filling pressure is hardly due to the LV dysfunction itself; they hypothesize that the changes in venous filling pressure are dictated by sympathetic control on venous capacity. The mechanism of a reduced venous capacity, yielding higher filling pressures to compensate for the impaired diastolic filling in the hypertrophied heart, is also supported by Safar and London (25).

Venous filling pressure is an important, sensitive modeling parameter (31). Small changes in absolute values are important in a relative sense and, therefore, have an important effect on pressure and flow. Venous filling pressure is explicitly introduced in the model, and we can only speculate on the (sympathetic) mechanisms controlling its value. We chose a mechanically driven feedback mechanism controlling venous filling pressure, i.e., normalization of wall stress, inasmuch as it is known that the heart muscle responds to mechanical stimuli. Alternatively, one may control venous filling pressure in such a way as to maintain cardiac output, but it is unknown whether the body contains flow or cardiac output sensors. In our simulations, both control mechanisms for venous filling pressure would yield very similar data, inasmuch as cardiac output is practically preserved in *scenario 3*.

Only ~10% of all hypertensive patients show clinical signs of LV hypertrophy, i.e., an increase in LV mass and relative wall thickness (9). This is also the patient subgroup with the highest total peripheral resistance and lowest total arterial compliance. Clinical observations suggest that, in hypertension, there is a relation between changes in arterial and cardiac mechanical and functional properties (6, 23, 35). We demonstrated that cardiac and arterial changes contribute to hypertension in LV hypertrophy. Consequently, it is important to consider the heart and the arterial system in the diagnosis, treatment, and follow-up of hypertension. In this study we used the model to simulate noninvasively measured data averaged over a control and a patient group. Similar analysis, with estimation of cardiac and arterial properties, is thus possible on a per-patient basis. The hemodynamic effect of alterations in these parameters is easily assessed, inasmuch as individual model parameters can be switched from control values to their actual patient values. This allows us to quantify the contribution of vascular vs. cardiac changes in hypertension to the increase of arterial blood pressure. Potentially, this approach may lead to a better prognostic marker for cardiovascular risk and to the use of more specific drugs in the treatment and follow-up of hypertensive patients.

This study, being a mathematical model study, inherently has some limitations. Although model results were compared with data measured invasively in patients with dilated cardiomyopathy, we could not validate our model in control subjects or in patients with concentric hypertrophy. Such data, consisting of simultaneously measured aortic pressure and flow and LV pressure and volume, are, to the best of our knowledge, not available. We focused on modeling the changes in the mechanical properties of the heart and the arterial system in concentric hypertrophy, without speculating on the molecular, genetic, and biochemical mechanisms triggering these changes in this complex, dynamic pathophysiological process (7). We further assumed linear end-diastolic and end-systolic P-V relationships, whereas they are curvilinear (4). We also modeled the arterial tree as a linear windkessel model, neglecting nonlinear pressure-dependent arterial properties. Furthermore, we modeled an increase in contractility in hypertrophy by an increase in LV wall thickness, also affecting passive diastolic properties and thus neglecting changes of intrinsic contractile myocyte properties (17, 20, 22).

In conclusion, on the basis of a mathematical heart-arterial interaction model, we have shown that concentric LV hypertrophy can be explained as a cardiac adaptation pattern to an increased afterload, in which peak systolic wall stress is normalized by increasing LV wall thickness, whereas an increased preload filling pressure compensates for the impaired diastolic filling and normalizes end-diastolic wall stress. The model predictions are in qualitative and quantitative agreement with in vivo findings on arterial pressure, cardiac output, and increase of LV mass. The proposed mechanisms may explain some of the ambiguity in the literature on whether peak systolic or end-diastolic LV wall stress is normalized. It should be realized however, that LV hypertrophy occurs only in ~10% of all hypertensive patients and that the model still cannot explain why some patients develop hypertrophy or how and why, in some hearts, hypertrophy is only an intermediate step toward heart failure.

We thank P. Steendijk for help and suggestions.

This research is funded by Zorgonderzoek Nederland PAD Project 97-23 and by a visiting professor grant from the Ecole Polytechnique Fédéralé de Lausanne.

REFERENCES

1. **Arts T, Bovendeerd PHM, Prinzen FW, and Reneman RS.** Relation between left ventricular cavity pressure and volume and systolic fiber stress and strain in the wall. *Biophys J* 59: 93–102, 1991.
2. **Banerjee A, Mendelsohn AM, Knilans TK, Meyer RA, and Schwartz DC.** Effect of myocardial hypertrophy on systolic and diastolic function in children: insights from the force-frequency and relaxation-frequency relationships. *J Am Coll Cardiol* 32: 1088–1095, 1998.
3. **Burkhoff D, Alexander J, and Schipke J.** Assessment of windkessel as a model of aortic input impedance. *Am J Physiol Heart Circ Physiol* 255: H742–H753, 1988.
4. **Burkhoff D, Sugiura S, Yue DT, and Sagawa K.** Contractility-dependent curvilinearity of end-systolic pressure-volume relations. *Am J Physiol Heart Circ Physiol* 252: H1218–H1227, 1987.
5. **Burkhoff D and Tyberg JV.** Why does pulmonary venous pressure rise after onset of LV dysfunction: a theoretical analysis. *Am J Physiol Heart Circ Physiol* 265: H1819–H1828, 1993.
6. **Chen C-H, Nakayama M, Nevo E, Fetics BJ, Maughan WL, and Kass DA.** Coupled systolic-ventricular and vascular stiffening with age. Implications for pressure regulation and cardiac reserve in the elderly. *J Am Coll Cardiol* 32: 1221–1227, 1998.
7. **Devereux RB and Roman MJ.** Left ventricular hypertrophy in hypertension: stimuli, patterns and consequences. *Hypertens Res* 22: 1–9, 1999.
8. **Douglas PS, Berko B, Lesh M, and Reichek N.** Alterations in diastolic function in response to progressive left ventricular hypertrophy. *J Am Coll Cardiol* 13: 461–467, 1989.
9. **Ganau A, Devereux RB, Roman MJ, de Simone G, Pickering TG, Saba PS, Vargiu P, Simongini I, and Laragh JH.** Patterns of left ventricular hypertrophy and geometric remodeling in essential hypertension. *J Am Coll Cardiol* 19: 1550–1558, 1992.
10. **Gelpi RJ, Pasipoularides A, Lader AS, Patrick TA, Chase N, Hittinger L, Shannon RP, Bishop SP, and Vatner SF.** Changes in diastolic cardiac function in developing and stable perinephritic hypertension in conscious dogs. *Circ Res* 68: 555–567, 1991.
11. **Grosman W, Jones D, and McLaurin LP.** Wall stress and patterns of hypertrophy in the human left ventricle. *J Clin Invest* 56: 56–64, 1975.
12. **Jin XY, Pepper JR, Brecker SJ, Carey JA, and Gibson DG.** Early changes in left ventricular function after aortic valve replacement for isolated aortic stenosis. *Am J Cardiol* 74: 1142–1146, 1994.
13. **Kelly RP, Tunin R, and Kass DA.** Effect of reduced aortic compliance on cardiac efficiency and contractile function of in situ canine left ventricle. *Circ Res* 71: 490–502, 1992.
14. **Lamb HJ, Beyerbacht HP, van der Laarse A, Stoel BC, Doornbos J, van der Wall EE, and de Roos A.** Diastolic dysfunction in hypertensive heart disease is associated with altered myocardial metabolism. *Circulation* 99: 2261–2267, 1999.
15. **Latson TW, Hunter WC, Burkhoff D, and Sagawa K.** Time sequential prediction of ventricular-vascular interactions. *Am J Physiol Heart Circ Physiol* 251: H1341–H1353, 1986.
16. **Li J.** Time domain resolution of forward and reflected waves in the aorta. *IEEE Trans Biomed Eng* 33: 783–785, 1986.
17. **Liu C-P, Ting C-T, Lawrence W, Maughan WL, Chang M-S, and Kass DA.** Diminished contractile response to increased heart rate in intact human left ventricular hypertrophy. Systolic vs. diastolic determinants. *Circulation* 88: 1893–1906, 1993.
18. **Mirsky I.** Left ventricular stresses in the intact human heart. *Biophys J* 9: 189–208, 1969.
19. **Monrad ES, Hess OM, Murakami T, Nonogi H, Corin WJ, and Krayenbuehl HP.** Time course of regression of left ventricular hypertrophy after aortic valve replacement. *Circulation* 77: 1345–1355, 1988.
20. **Morii I, Kihara Y, Moriaki I, and Sasayama S.** Myocardial contractile efficiency and oxygen cost of contractility are preserved during transition from compensated hypertrophy to failure in rats with salt-sensitive hypertension. *Hypertension* 31: 949–960, 1998.
21. **Murgo JP, Westerhof N, Giolma JP, and Altobelli SA.** Aortic input impedance in normal man: relationship to pressure wave forms. *Circulation* 62: 105–116, 1980.
22. **Nguyen TN, Chagas ACP, and Glantz SA.** Left ventricular adaptation to gradual renovascular hypertension in dogs. *Am J Physiol Heart Circ Physiol* 265: H22–H38, 1993.
23. **Pierdomenico SD, Lapenna D, Guglielmi MD, Porreca E, Antidormi T, Cuccurullo F, and Mezzetti A.** Vascular changes in hypertensive patients with different left ventricular geometry. *J Hypertens* 13: 1701–1706, 1995.
24. **Randall OS, Van Den Bos GC, and Westerhof N.** Systemic compliance: does it play a role in the genesis of essential hypertension? *Cardiovasc Res* 18: 455–462, 1984.
25. **Safar ME and London GM.** Arterial and venous compliance in sustained essential hypertension. *Hypertension* 10: 133–139, 1987.
26. **Sasayama S, Franklin D, and Ross J Jr.** Hyperfunction with normal inotropic state of the hypertrophied left ventricle. *Am J Physiol Heart Circ Physiol* 232: H418–H425, 1977.
27. **Schreuder JJ, van der Veen FH, van der Velde ET, Delahaye F, Alfieri O, Jegaden O, Lorusso R, Jansen JRC, Hoeksel SA, Finet G, Volterrani M, Kaulbach H-G, Baan J, and Wellens HJJ.** Left ventricular pressure-volume relationships before and after cardiomyoplasty in patients with heart failure. *Circulation* 96: 2978–2986, 1997.
28. **Senzaki H, Chen C-H, and Kass DA.** Single-beat estimation of end-systolic pressure-volume relation in humans. A new method with the potential for noninvasive application. *Circulation* 94: 2497–2506, 1996.
29. **Shannon RP, Komamura K, Stambler BS, Bigaud M, Manders WT, and Vatner SF.** Alterations in myocardial contractility in conscious dogs with dilated cardiomyopathy. *Am J Physiol Heart Circ Physiol* 260: H1903–H1911, 1991.
30. **Simon AC, Safar ME, Levenson JA, London GM, Levy BI, and Chau NP.** An evaluation of large artery compliance in man. *Am J Physiol Heart Circ Physiol* 237: H550–H554, 1979.
31. **Stergiopulos N, Meister JJ, and Westerhof N.** Determinants of stroke volume and systolic and diastolic pressure. *Am J Physiol Heart Circ Physiol* 270: H2050–H2059, 1996.
32. **Stergiopulos N, Meister JJ, and Westerhof N.** Simple and accurate way for estimating total and segmental arterial compliance: the pulse pressure method. *Ann Biomed Eng* 22: 392–397, 1994.
33. **Stergiopulos N, Westerhof B, and Westerhof N.** Total arterial inertance as the fourth element of the windkessel model. *Am J Physiol Heart Circ Physiol* 276: H81–H88, 1999.
34. **Suga H, Sagawa K, and Shoukas AA.** Load independence of the instantaneous pressure-volume ratio of the canine left ventricle and effects of epinephrine and heart rate on the ratio. *Circ Res* 32: 314–322, 1973.
35. **Sumimoto T, Mukai M, Murakami E, Kokubu T, Lin M, Shigematsu Y, Hamada M, and Hiwadi K.** Effect of age on left ventricular geometric patterns in hypertensive patients. *J Hypertens* 13: 1813–1817, 1995.
36. **Toorop GP, Westerhof N, and Elzinga G.** Beat-to-beat estimation of peripheral resistance and arterial compliance during pressure transients. *Am J Physiol Heart Circ Physiol* 252: H1275–H1283, 1987.